Current Pharmaceutical Biotechnology, 2018, *19*, 1005-1013

RESEARCH ARTICLE

Improving Bovine Bone Mechanical Characteristics for the Development of Xenohybrid Bone Grafts

Alberto Cingolani[1,2], Carlo Francesco Grottoli[2], Raffaella Esposito[3], Tomaso Villa[3], Filippo Rossi[4] and Giuseppe Perale[2,5,6*]

[1]*Department of Chemistry and Applied Bioscience ETH Zurich, Institute for Chemical and Bioengineering, Vladimir-Prelog-Weg 1-5/10, 8093 Zürich, Switzerland;* [2]*Industrie Biomediche Insubri SA (IBI), Via Cantonale 67, 6805 Mezzovico-Vira, Switzerland;* [3]*Laboratory of Biological Structure Mechanics, Department of Chemistry, Materials and Chemical Engineering "G. Natta", Politecnico di Milano, 20133 Milan, Italy;* [4]*Laboratory of Applied Physical Chemistry, Department of Chemistry, Materials and Chemical Engineering "G. Natta", Politecnico di Milano, 20133 Milan, Italy;* [5]*Biomaterials Laboratory, Institute for Mechanical Engineering and Materials Technology, SUPSI – University of Applied Sciences and Arts of Southern Switzerland. Via Cantonale 2C, Galleria 2, 6928 Manno, Switzerland;* [6]*Department of Surgical Sciences, Orthopaedic Clinic-IRCCS A.O.U. San Martino, 16132 Genova, Italy*

Abstract: ***Background***: The further functionalization of natural existing biomaterials is a very efficient method to introduce additional advanced characteristics on a unique structural composition and architecture.

Objective: As an example, different animal sources, if properly treated, can be used to develop bone xenograft active in hard tissues regeneration. In this sense, it is also important to consider that the selected process has to take into consideration the intrinsic variability of the base material itself and possibly being able to compensate for it.

Methods: In this work we characterize cancellous bovine bone treated by deposition of polymer and collagen and we show that the added components not only lead to a more resistant and more hydrophilic material, but also reduce the conventional correlation between apparent density and elastic modulus, which, in general, is a major source of uncertainty and risk in xenografts usage.

Results: Moreover, though intrinsically reinforcing the material, the deposition process leaves the specific open-porous structure, that allows cells proliferation and vessels ingrowth, basically unaltered.

Conclusion: The final material combines in a single piece and at the same time, mechanical resistance, homogeneous mechanical response and proper structural characteristics that allow further integration within the patient autochthonous tissues.

ARTICLE HISTORY

Received: June 19, 2018
Revised: September 03, 2018
Accepted: November 25, 2018

DOI:
10.2174/1389201020666181129115839

Keywords: Hard tissues regeneration, xenografts, tissue engineering, biomaterials, bovine bone, biopolymers.

1. INTRODUCTION

As recent studies and characterization at nano and micro-scale of biological complex systems enabled to enlighten and understand the mechanism of action of many of them [1], novel and elaborated multi-functional materials, mimicking [2, 3] or taking inspiration [4] from their natural counterparts started to be properly developed and implied in diverse engineering strategic fields, from surface [5] and structure design [6] to tissue regeneration [7-10]. In most biological materials the advanced peculiarities are provided by the unique structural composition, both in terms of chemistry as well as physical arrangement, which is, in general, obtained following a naturally occurring bottom-up approach [11]. A very good example, in this sense, is represented by the biomineralization processes leading to complex hierarchical structures [12]. It appears evident that replicating or externally guiding the development of such a refined solid framework in three dimensions, is all but trivial and, most of the time, highly

*Address correspondence to this author at Biomaterials Laboratory, Institute for Mechanical Engineering and Materials Technology, SUPSI – Universityof Applied Sciences and Arts of Southern Switzerland. *Via* Cantonale 2C, Galleria 2, 6928 Manno, Switzerland; Tel: +41919306640;
Fax: +41912207200; E-mail: giuseppe.perale@supsi.ch

1873-4316/18 $58.00+.00

complicated strategic paths and methodologies need to be properly devised [3, 13, 14]. Moreover, most biological materials do not have only one functionality, but rather a combination of different ones and need to be treated as composites. Indeed, *e.g*. in biomaterials intended for bone grafting and substitution, a mineral or ceramic component is needed to provide strength and stiffness whereas other biopolymer constituents are needed to provide the viscoelastic damping and toughness while also offering enhanced cell viability [1, 15].

Another possibility that allows the overcoming of the aforementioned difficulties in synthetic strategies, is represented by the utilization of already naturally existing biomaterials, either directly or after a post-treatment providing additional advanced functionalities [16, 17]. Certainly, bone-grafts obtained from animal-derived cancellous bone, and implied as substitutes and filler in hard tissue regeneration, represent a major category in this sense, also being routinely used in clinical practice ever since many decades [18, 19]. Indeed, autografts (when the bone comes from the patient itself) as well as allografts (when the bone comes from another human donor, either living or cadaver) and xenografts (when the bone comes from an animal) have been all successfully applied in bone repair, in a wide spectrum of reconstructive surgical specialties [20]. It is acknowledged that bovine-derived cancellous bone grafts are the closest xenograft to human bone to be regenerated, second self-evidently only to autografts [21-23]. These biomaterials clearly present a major advantage over their synthetic competitors (*e.g*. hydroxyapatite, beta-TriCalciumPhospate, *etc.*), since they have much higher osteogenic and osteoconductive performances [16, 20, 24]. Indeed, the hierarchical porous structure [25], naturally present in cancellous bone, acts as a scaffold for cells favoring their colonization and proliferation [20]. This way, the implanted device gets completely integrated into the body and over long periods completely replaced by the patient autochthonous tissues [16]. However, necessary cleaning and sterilization processes of starting raw materials of animal origin result in a decay of both mechanical and biological performances. Moreover, when dealing with naturally produced biomaterials, it is always necessary to keep in mind that they arise from processes which preserve an intrinsic biological variability in the final product [1]. This concept is both valid for materials coming from equivalent part, but different individual systems (*i.e*. the bone of the same part of two bovines of the same species) as well as for distinct section within the same one (the bone between the different segments of the same animal). Focusing on bovine-derived bone xenografts, it is well known that the density of cancellous bone varies along trabecular trajectories with a major consequence on its mechanical properties [23, 26]. Therefore, in the frame of using it as a base material for the development of implantable devices, which need to meet both requirements of tissue regeneration and structural support, this represents a huge limitation. As a matter of fact, the lack of possibility of predicting a priori, the mechanical response to the applied load once placed inside the patient body generates a high risk that should be mitigated, also according to new regulatory framework requirements [27]. Consequently, in order to make animal-derived cancellous bone, a desirable material for bone grafts, a technique not only improving but also homogenizing the mechanical properties, making them independent on the raw, untreated material characteristics, is required [23]. Last but not the least, the actual porous structure needs to be left open, interconnected and very poorly altered to preserve the osteogenic and osteoconductive performances [23]. Indeed, similar to what has been commonly seen for synthetic biomaterials [23], the application of composite technologies to bovine xenografts is becoming an interesting trend, not only in research [28, 29] but also in industrial and clinical practices [17, 30]: the addition of resorbable polymeric components improves mechanical and biological performances [10] and can also be used to locally carry active molecules, or drugs to be delivered locally, to increase cell colonization, promote osteoinduction and finally promote osteogenesis [16, 24]. Overall, increased performance of bone graft is still the major focus in orthobiologics [23].

Within this framework, we here present the characterization of a material developed upon treatment of cancellous decellularized, deproteinized and defatted bovine bone with additional biopolymer and collagen fragments [17] in order to track the effect of the post-modification on the final product. It was found that the treatment not only improves considerably the mechanical properties and hydrophilicity of the initial bovine-derived matrix, but rather makes them more independent of the intrinsic porous structure, overcoming the difficulties of using a nonuniform base material.

Single 15x30x60mm^3 pieces of cancellous bovine bone, biggest harvestable from adult bull femur head, have been subdivided in the different subsections which have been individually analyzed before and after the treatment. If the mechanical properties, as expected, were highly dependent on the density of the raw material, a considerable homogenization of them is instead recorded after modification, together with an overall increased mechanical resistance. In addition, the conventional porous structure is not modified, and very similar density and porosity values are recorded before and after the treatment. The combination of these two concepts is of utmost importance: on the one hand, the homogenous mechanical response is ensured; on the other hand, cells proliferation and vascular ingrowth are not hindered by changes in the porous structure, being even further enhanced by the presence of collagen fragments [24]. As a matter of fact, the characteristics of the final product support it in being a proper xenograft, able to be not only effectively implanted but also fully substituted by patient living healthy bone [16, 30].

2. MATERIALS AND METHODS

2.1. Materials

Among modified xenografts, a scaffold composed of processed bovine bone matrix, mainly mineral constituted, reinforced with biopolymers, namely block copolymer of poly(L-lactic acid) and poly(ε-caprolactone), with selected physical properties to allow proper withstanding of treatment and sterilization [31], and arginylglycylaspartic acid (RGD) containing collagen fragments (mainly type I), obtained from animal-derived gelatin [32], has recently been proposed as a bone substitute for reconstructive surgeries, available as a

class III medical device (commercially named SmartBone®, by Industrie Biomediche Insubri SA, Switzerland) [16, 17, 24, 30]. Bovine-derived decellularized, defatted and deproteinized cancellous bone is sourced certified for human use and of BSE/TSE (Bovine Spongiform Encephalopathy/ Transmissible Spongiform Encephalopathies) free origin (currently "Negligible BSE risk Countries", former "OIE1 Countries").

2.2. Cutting of the Bone and Reinforcement Process

Raw bovine bone blocks used in this study present a nominal size of 15x30x60mm^3. Before applying reinforcement with biopolymers and collagen, each block was subdivided into smaller identical cubes of nominal dimension of 7x7x7mm^3 by properly cutting the initial shape with a diamond-edged automatic saw. The reason for which the sum of the length of the individual cubes is smaller than the total one of the initial block resides in the thickness of the blade that indeed consumes roughly 1.5 mm when cutting. During this phase, the bone was wet with water and ethanol in order to minimize temperature increase, due to friction, and dust generation. Proper sizing of the samples was measured with a digital calibrated caliber with a resolution of 0.05 mm (Adolf Würth GmbH & Co. KG, Germany).

Once oven dried (in vacuum at 37°C for 18 h), the obtained cubes (56 per each starting block, see also scheme depicted in Fig. **3**) had been treated with the proprietary reinforcement process that allowed deposition, over the bone surfaces, of biopolymers embedding animal-derived gelatin that allows RGD-containing collagen fragments [17, 33, 34]. This process involves: a) preparation of a solution of reinforcing mixture containing a dissolved polymer and gelatin b) immersion of the base matrix and c) drying in a vacuum oven at 37°C for 24 h for removing possible solvents residues.

2.3. Physical-chemical Characterization

Each individual sample has been weighted and measured using an electronic calibrated balance Mark 8055 (Bel Engineering, Monza, Italy) and digital caliber with a resolution of 0.05 mm (Adolf Würth GmbH & Co. KG, Germany) before and after the treatment. Apparent density has been determined by the classical definition of mass over volume. The volume was computed using the conventional geometrical formulas for parallelepiped solids (L1xL2xL3). For the measurement of the contact angle and wetting properties, pictures of the drops were taken using a digital microscope AM4115T from Dino-lite (AnMo Electronics corporations, Taiwan). The actual values have been computed using Image J software [35, 36]. The reported values are averaged over five independent measurements. Environmental scanning electron microscopy (ESEM) and energy dispersive analysis (EDS) were performed at 10 kV with 50 EP Instrumentation (Zeiss, Jena, Germany), according to previously published methodology [34], to assess the correct presence of the polymeric domains. FTIR analysis has been performed as follows: samples were laminated with potassium bromide and then recorded using a Thermo Nexus 6700 spectrometer coupled to a Thermo Nicolet Continuum microscope equipped with a ×15 Reflachromat Cassegrain objective.

2.4. Mechanical Tests and Analysis of the Data

According to previously published methodology [34], compression tests were run on MTS 858 MiniBionix testing machine (S/N 1015457, MTS, Minneapolis, MN, USA) driven by a digital controller Test Star II. The machine was equipped with a hydraulic axial actuator with a load capacity of 25 kN and an LVDT displacement transducer with a working range of 100 mm. The compression tests were run after placing the specimen in the lower center of the two rigid parallel steel plates, connected to the load cell of the testing machine: the upper plate, connected to the actuator of the same machine, was then moved downward at 1 mm/min speed under displacement control. The test was stopped when the maximum load peak was reached. During the test, force and displacement data were collected at 10 Hz frequency: the data were then elaborated to obtain the stress σ on a generical section S computed as $\sigma = F / S$, where F is the actual force measured by the load cell. Moreover, the strain of the specimen was calculated as $\varepsilon = \Delta L / L_0$, where L_0 is the initial height of the sample in the direction of the test and ΔL is the measured value of the actuator displacement equivalent to the shortening of the specimen during the test. These data were used to build, for each individual sample, the stress-strain plot, from which the elastic modulus E was obtained as the initial linear slope of the curve. Experimental data were analyzed using Analysis of Variance (ANOVA); statistical significance was set to P value < 0.05. Results are presented as mean $\pm$ standard deviation.

3. RESULTS AND DISCUSSION

3.1. Intrinsic Variability in Untreated Pristine Cancellous Bone Tissues

As generally known and already discussed by Langton *et al*. [25] and Skedros *et al*. [26], cancellous bone has a non-uniform porous structure, whose internal arrangement depends indeed on many factors, including position within the body, functions and applied loads [37]. Moreover, bone experiences continuous re-shaping also during an individual's life and changes its structure continuously depending on the external stimuli, which include diet, diseases, traumas and lifestyle [38, 39]. Fig. (**1**) shows the top view of a decellularized cancellous bovine block as purchased to manufacture SmartBone®. Clearly, different trajectories can be identified within the constituting trabeculae and, already by visual inspection, major differences in porosity are visible over the whole volume of the block itself. This reflects also in high apparent density gradient along the block body with a consequential contiguous variation of the mechanical characteristics as well. Although a correlation between these two aforementioned parameters exists and is well established [40], one has to be very careful in using it. Indeed, as shown in Fig. (**1** and **2**), over a huge volume of bone (in this case 15x30x60mm3, being the biggest harvestable cancellous bone block from an adult femur head) some areas might be considerably denser than the others with the consequence of having regions which have different resistance. Therefore, the overall apparent density might be not really representative of the distribution of mechanical properties within the block. This previous statement becomes even more im-

portant when considering that, in general, the block would not be used as such but rather properly cut or milled to reach complex geometries to be adapted to fit into real bone defects. As a matter of fact, hardly it is possible to find a contiguous way through the bone presenting homogeneous structure and eventually also the finished piece will have inevitably a substantial inhomogeneity in its final properties, even different from the ones of the initial block itself, as depicted in Fig. (**2**). This represents a huge limitation for an implantable device, especially considering that it is often very difficult to know in advance where exactly and in which conditions, the piece will be placed into the patient body and which loads it will have to withstand over a long period of time. In order to properly rationalize what previously discussed, we decided to investigate and identify the actual density gradient of the bone blocks and establish in which way it affects the distribution of mechanical properties in the untreated, pristine bovine bone. Apart from the already introduced intrinsic variability of the bone itself, related to its animal origin, it is also true that visually all blocks present a similar trabecular pattern, with defined orientation of the trabecular paths, being related to harvesting made when extracting raw materials from adult male cattle. Indeed, coming from a bovine femur's head, they present a trajectorial structure, which enables to roughly identify the orientation of the block within the initial femur's matrix, following Wolff trajectory hypothesis [41]. The obtained value is 40° over the plane tangential to the femur's head. Moreover, it is important to state that there are not too many lines over which the cut can be applied in order to obtain such a huge volume of bone in a single shape, with the best possible homogeneity. This statement is also confirmed by the supplier, who ensure identical shaping conditions and cutting orientation for all his products, being a medical device manufacturing process. The initial blocks, therefore, have been first split into two halves, the top one named ***v*** and the bottom named ***o***. Subsequently, both of them have been also parted into four smaller sections along the longer side, named A, B, C and D. In order to obtain representative values, these four sections have also been subdivided into seven pieces each, obtaining cubes of 7x7x7mm^3, as previously described and shown in Fig. (**3**). Each of these pieces has been characterized individually in terms of density and mechanical properties and average values for each of the four sections obtained. In this sense, only variation in average density of at least 0.01 g/cm^3 has been considered relevant in the frame of an accurate quantification of the difference before and after the treatment. Moreover, since in general bone is anisotropic [25], it was decided to apply a vertical load to the pieces coming from section ***v*** and a horizontal one to those coming from ***o***, in order to obtain a more complete and more statistically robust characterization [42].

3.1.1. Apparent Density

As mentioned before, there is a substantial difference in measuring the apparent density of the block as a whole and of its diverse sections. The results are reported in Fig. (**4**) and it can be seen that density increases moving from section A to D over the whole block volume in both sections ***v*** and ***o***. Moreover, though the trend is the same, some difference is observed also between the top and the bottom of the block itself. Therefore, it can be stated that the density, and therefore the porosity, of the block varies both in the horizontal as well as vertical axis of the block. On the other hand, though the recorded values are not homogeneous, they all ensure the right porosity and arrangement for cell colonization of the support, being a matching result with the orthobiologics' main paradigm.

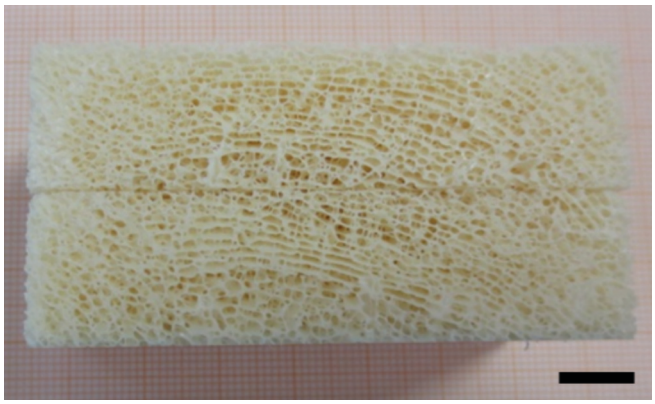

Fig. (1). Top view of the prisitne cancellous bovine bone (scale bar = 10 mm), showing the trabecular arrangement and the consequent porous structure.

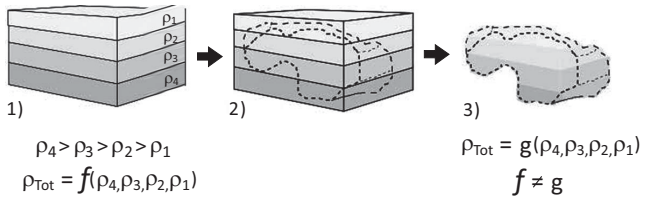

Fig. (2). General scheme of the usage of the block for the preparation of derived products. 1) An initial block of bone presents a gradient of density along its volume. Each different sector, with his own density contribute to overall density of the block. When the block is milled and shaped in complex geometries 2), it is often hard to be able to work only within a section with homogenous density, with the result 3) that the final piece might have a different density distribution along its volume.

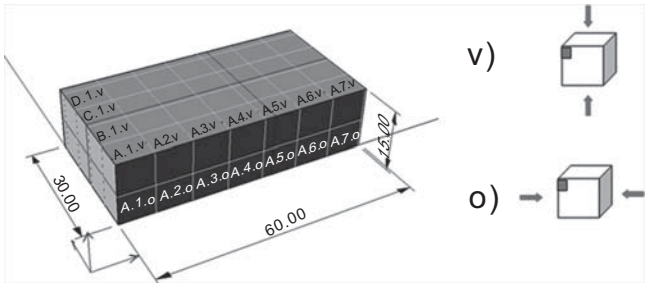

Fig. (3). Subdivision of the block into smaller sections and individual pieces. On the top section v the load has been applied vertically whereas on the bottom one o, horizontally.

3.1.2. Mechanical Properties

The analysis of mechanical properties reveals a substantial, yet expected, dependence of the elastic modulus E on the apparent density of the tested cubic sample, as reported

in Fig. (**5**). Moreover, moving from section A to D, in both part ***v*** and ***o***, a clear gradient in the value of E can be noticed. In general, the higher is the density, the higher the mechanical resistance, independently of the direction over which the load is applied. In particular, the value of E moves from 258.07 ± 72.8 MPa to 518.2 ± 76.4 MPa in the case of applied horizontal load and from 182.94 ± 70.5 MPa to 410.45 ± 64 MPa for the vertical one. As a matter of fact, it can be easily observed that the huge variability of the apparent density within the different section, reflects in a similar variability on the mechanical properties of the untreated material. For the sake of completeness, it is important to remind that the apparent density is not the only parameter affecting the elastic modulus value, but also many others, such as the trabeculae orientation and the actual position of the bone within the body might have an impact. In our specific case, the obtained values find good accordance with those reported by Töyräs *et al.* [43] who measured an elastic modulus of 278 ± 154 MPa for a femur's head and 495 ± 245 MPa for a bovine tibia.

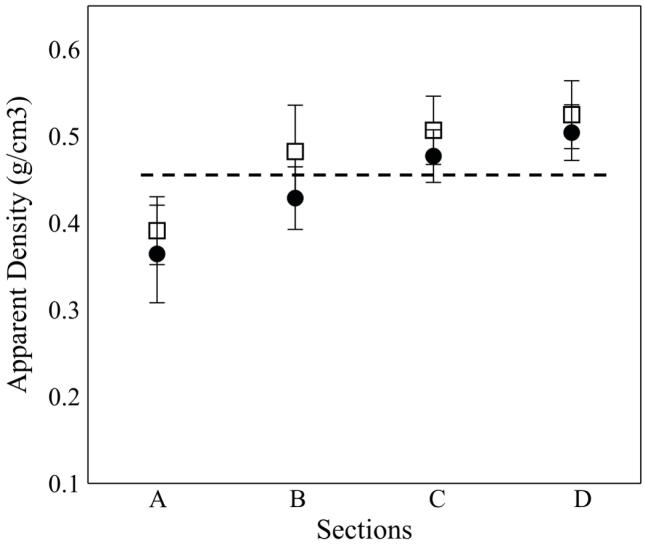

Fig. (4). Apparent density within the different block sections (A,B,C,D) for the pristine bone block, both in the v part (●) as well as o one (□). In addition, also the overall apparent density of the block is plotted (dashed line).

3.2. Effect of the Reinforcement Treatment

In this section, the effect of the treatment on the previously investigated physical and structural characteristics of the initial matrix is evaluated. As mentioned before, the process basically involves the deposition of polymer (PLA-PCL) and gelatin on the pristine cancellous bovine-derived bone. The first component provides elasticity and toughness and limits the otherwise fragile behavior of the bone. The second one improves hydrophilicity and ensures good cell adhesion and viability [34]. The block has been first subdivided in sections and pieces following the same procedure as before. Afterward those samples have been treated and characterized in the same way as the untreated ones. As already highlighted, because of equivalent cutting angle and procedure directly out of the femur's head, good correspondence is found within the orientation of the trabecular frame among the two used starting blocks. This visual check makes the obtained results, despite very little intrinsic variability, properly and reasonably comparable.

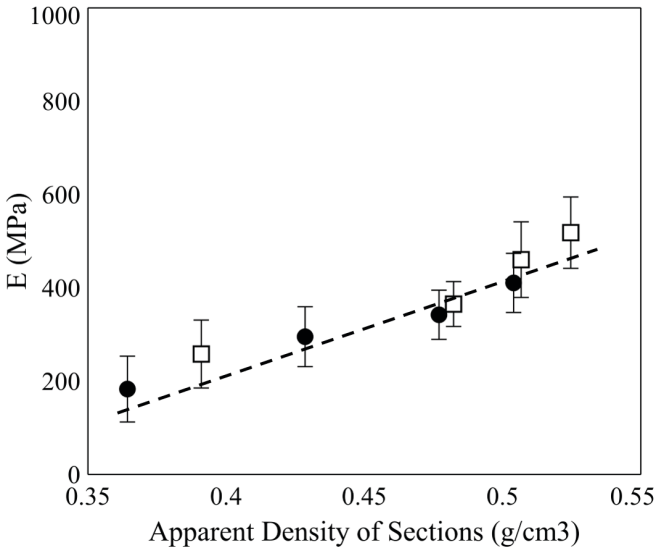

Fig. (5). Elastic modulus vs density of the prisitne bone block, for the vertical applied load (●) and the horizontal one (□). For the apparent density, average values have been reported. The dashed line is plotted for trend evidencing only.

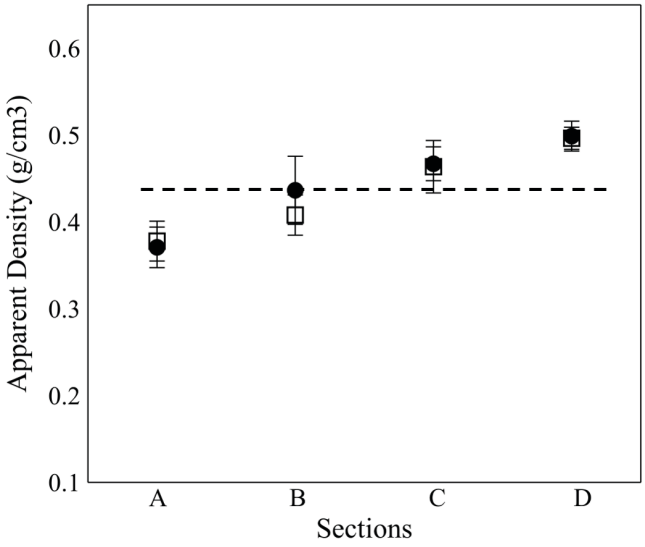

Fig. (6). Apparent density within the different block sections (A,B, C,D) for the treated bone block, both in the v part (●) as well as o one (□). In addition, also the overall apparent density of the block is reported (dashed line).

3.2.1. Apparent Density

As it can be seen from Fig. (**6**), after the reinforcement treatment, a trend very similar, with even properly similar density values, is observed for the case of the treated block with respect to untreated ones. Therefore, the intrinsic variability of untreated bone among the different sections is preserved. In light of these results, indeed, to make sure that

polymer and gelatin are actually present on the treated bone surfaces, two additional measurements have been run. In Fig. (**7**), an example of two contact angle measurements of water in the air over the surface of the untreated (left) and treated (right) bone are reported. Though hydroxyapatite is in general hydrophilich [44] due to the porosity of the surface (Cassie-Baxter mode [45-47]) an apparent hydrophobic behavior is recorded before the treatment, with apparent contact angle of 100° ± 4°, whereas, after it, a rather hydrophilic one with contact angle of 69° ± 15° after 6 seconds. Moreover, it is important to mention that, if no changes in drop displacement were observed for the untreated samples, often a full water penetration within the bone porous domain was recorded over longer times for the treated ones. Gelatin is well known and used in drug formulation [48] for its water absorption and swelling ability. It is therefore not surprising that its presence, even in small amount, on the bone surface, leads to enhanced hydrophilicity and water absorption capacity. This makes the xenograft also more accessible from the patient's blood upon implantation, favoring cells colonization and vascular ingrowth [16].

In addition, the ESEM pictures in Fig. (**8.a** and **8.b**) show the presence of deposited material (darker part) within the internal surface of the pores, while the energy dispersive analysis (Fig. **8.c** and **8.d**) reveals difference within the relative abundance of atomic species in different sections of the treated bone. Specifically, in the darker area, a much higher presence of carbon atoms, due to the polymer composition, is detected. These results have also been confirmed *via* FTIR analysis (Fig. **S1**), in which clearly peaks corresponding to -OH (3450 cm^{-1}), -CH_3 (2960 cm^{-1}), carbonyl (1640 cm^{-1}) and C-O-C (1100 cm^{-1}) bonds are detectable after treatment, whereas before only the ones corresponding to the mineral nature of the samples are present (1050 and 600 cm^{-1}). Therefore, it is confirmed that polymer and gelatin are effectively deposited over the starting bone matrix. Though the involved quantities are not enough to affect the apparent

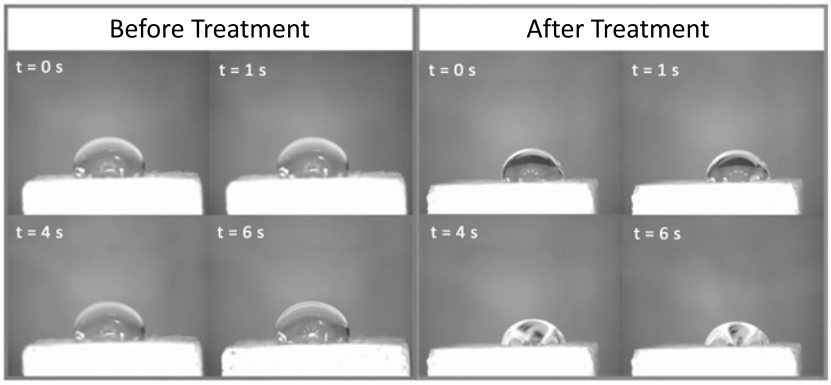

Fig. (7). Displacement of a water droplet at different instants on the surface of the prisitne bone (left) and after the treatment (right). Actual values of contact angle have been measured for both cases on the picture in the last square (t = 6 s), as afterwards no further changing in the displacement of the drop over the surface was recorded. Specifically, for the shown case of the pictures before the tratement (left) the recorded angle is 103° ± 6° and afterwards (right) 73° ± 4°.

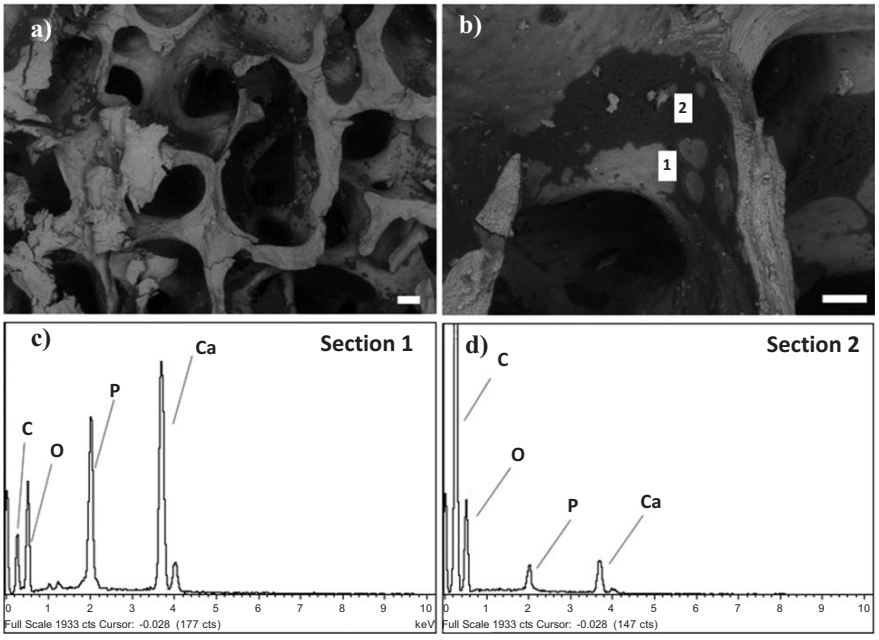

Fig. (8). ESEM pictures of the bone after the treatment, at different magnifications. For a, scale bar = 200 μm and for b with scale bar = 100 μm. c) and d) are the energy dispersive analysis of the two different sections, c of the lighter (1) and d for the darker one (2) in b.

density of the samples they are, on the contrary, enough to modify some other physical properties and to relevantly influence biological behavior and hence clinical performances [24, 30].

3.2.2. Mechanical Properties

As one can see from Fig. (**9**) the effect produced by the deposited materials on the pristine bone matrix can be subdivided in two major points. First, it increases the mechanical resistance of the actual sample, moving the values of E towards considerably higher ones, specifically from an average value of 384.46 ± 124.8 MPa to one of 461.49 ± 66.5 MPa for section ***v*** and from 485.17 ± 63.66 MPa to 531.5 ± 82.3 MPa for section ***o***. This represents an improvement of roughly 27% over the initial material in the ***v*** section and of 25% in the ***o*** one. As the polymer and gelatin properly stick on the bone support, certainly there is a contribution of adhesion forces to the observed structural reinforcement. Moreover, the presence of a polymer phase, even in very low amounts, significantly stabilizes crack propagation within the mineral matrix. With dependence on the polymer characteristics, toughening (if the polymer is soft) and increased mechanical strength (if the polymer is stiff) can be provided. Additionally, the toughness of the polymer phase itself also contributes to the enhanced mechanical response of the composite material.

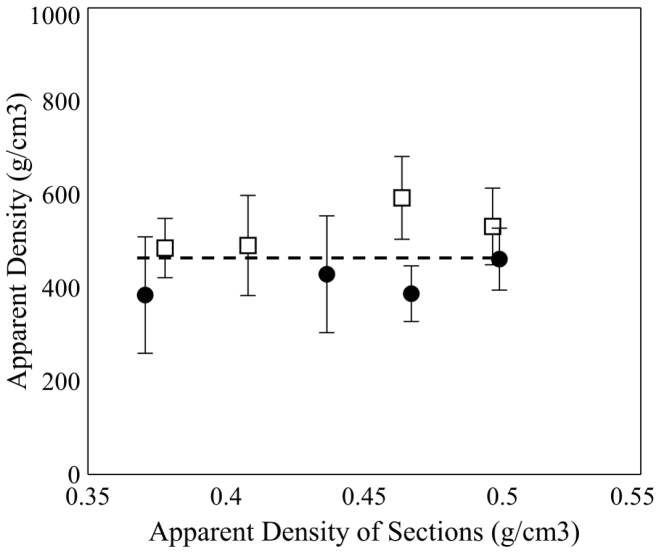

Fig. (9). Elastic modulus vs the apparent density of the different sections of the treated bone block, for the vertical applied load (●) and the horizontal one (□). For the apparent density, average values have been reported. The dashed line is plotted for trend evidencing only.

Considering the characteristics of our polymer, which at room temperature is a very though, rubbery-like solid (T_g = 16°C; E = 200 MPa, tensile strength = 240 N/mm^2; strain at failure = 160%), such an improvement is expected when even only traces are deposited on the pristine bone, as already observed for similar systems, like nacre-like materials[6]. Moreover, as already discussed by Chen [40], protein and mineral constituents of the bone at micro and nano-scales may interpenetrate, thus enhancing the mechanical properties by interlocking [49]. Indeed, in general, as soon as natural bone is deproteinized its mechanical properties fall considerably and it presents a rather fragile and brittle behavior [40]. Secondly, the treatment considerably homogenates the actual mechanical response over the different sections of the block, once again independently on the direction of the applied load, lowering substantially the dependence of the elastic modulus on the apparent density. This, again, can be explained by the effect of the polymer presence within the trabeculae of the original matrix, generating a more homogeneous stress distribution, limiting stress concentration at the mineral bridges [6, 50].

Mechanical properties hence become much more distributed over the body of the block and/or any other complex volume therefrom extracted, limiting consistently the intrinsic variability of such a peculiar base material. Notably, as in most composite materials, even a small amount of polymer and gelatin incorporation is enough to provide proper additional strength. Moreover, being the deposition process controlled by the affinity of polymer and gelatin for the bone support itself, it can be expected that on samples with higher porosity, and therefore, more surface area a higher quantity of material is deposited with a more relevant effect on the reinforcement. Remarkably, as already shown before, the apparent density of all samples is only minimally affected by the process and the peculiar structure ensuring cell colonization is preserved [51].

CONCLUSION

In this work, we have characterized deproteinized and decellularized cancellous bovine bone before and after the deposition of polymer and gelatin. This way, we have shown that its mechanical properties can be improved and homogenized. Specifically, the added components not only lead to a more resistant material, but also, they allow the overcoming of an intrinsic, naturally occurring limitation in pure bovine cancellous bone characteristics. Indeed, the conventional correlation between apparent density and elastic modulus, the major source of uncertainty and risk of poor outcomes in the possible usage of pure xenografts in bone tissue engineering, is considerably reduced on the samples that underwent the treatment. Combined with the enhanced hydrophilicity provided by the gelatin, the presented biohybrid composite stands as one of the best candidates for hard tissue integration and regeneration practice. Indeed, though intrinsically reinforcing the material, the deposition process leaves the specific porous structure, that allows cells proliferation, basically unaltered. As a matter of fact, the final material presents many advantages as it combines and address in a single piece and at the same time mechanical resistance, homogeneous mechanical response and proper structural characteristics[51] that allow full integration within the patient receiving site tissues and complete tissue remodeling [16].

ETHICS APPROVAL AND CONSENT TO PARTICIPATE

Not applicable.

HUMAN AND ANIMAL RIGHTS

No Animals/Humans were used for studies that are the basis of this research.

CONSENT FOR PUBLICATION

Not applicable.

CONFLICT OF INTEREST

Prof. Dr. Giuseppe Perale is one of the owners of the proprietary process involved in the preparation of the samples, executive vice president and a co-founder of the company IBI SA using that technology. Dr. Alberto Cingolani and Ing. Carlo Grottoli also work for the same company.

ACKNOWLEDGEMENTS

The authors are very thankful to Arnaldo Varesti for his kind help with the preparation of the samples and the usage of the microscope. Moreover, they would like to express their gratitude to Dario Picenoni for the ESEM measurements. Many thanks also to Marco Binelli for the FTIR measurements.

SUPPLEMENTARY MATERIAL

Supplementary material is available on the publisher's website along with the published article.

REFERENCES

[1] Chen, P.Y.; McKittrick, J.; Meyers, M.A. Biological materials: Functional adaptations and bioinspired designs. *Prog. Mater. Sci.,* **2012**, *57*(8), 1492-1704.

[2] Espinosa, H.D.; Juster, A.L.; Latourte, F.J.; Loh, O.Y.; Gregoire, D.; Zavattieri, P.D. Tablet-level origin of toughening in abalone shells and translation to synthetic composite materials. *Nat. Commun.,* **2011**, *2*(1), 173-179.

[3] Yeom, B.; Sain, T.; Lacevic, N.; Bukharina, D.; Cha, S.H.; Waas, A.M.; Arruda, E.M.; Kotov, N.A. Abiotic tooth enamel. *Nature,* **2017**, *543*(7643), 95-98.

[4] Launey, M.E.; Munch, E.; Alsem, D.H.; Barth, H.B.; Saiz, E.; Tomsia, A.P.; Ritchie, R.O. Designing highly toughened hybrid composites through nature-inspired hierarchical complexity. *Acta Mater.,* **2009**, *57*(10), 2919-2932.

[5] Yang, H.; Liang, F.; Chen, Y.; Wang, Q.; Qu, X.; Yang, Z. Lotus leaf inspired robust superhydrophobic coating from strawberry-like janus particles. *NPG Asia Mater.* **2015**, *7*(4), e176.

[6] Niebel, T.P.; Bouville, F.; Kokkinis, D.; Studart, A.R. Role of the polymer phase in the mechanics of nacre-like composites. *J. Mech. Phys. Solids,* **2016**, *96*, 133-146.

[7] Santoro, M.; Perale, G. Using synthetic bioresorbable polymers for orthopedic tissue regeneration. *Durab. Reliab. Med. Polym.,* **2012**, 119-139.

[8] Sheikh, Z.; Najeeb, S.; Khurshid, Z.; Verma, V.; Rashid, H.; Glogauer, M. Biodegradable materials for bone repair and tissue engineering applications. *Materials (Basel),* **2015**, *8*(9), 5744-5794.

[9] Stevens, B.; Yang, Y.; Mohandas, A.; Stucker, B.; Nguyen, K.T. A review of materials, fabrication methods, and strategies used to enhance bone regeneration in engineered bone tissues. *J. Biomed. Mater. Res. - Part B Appl. Biomater.,* **2008**, *85*(2), 573-582.

[10] Rossi, F.; Santoro, M.; Perale, G. Polymeric scaffolds as stem cell carriers in bone repair. *J. Tissue Eng. Regen. Med.,* **2015**, *9*, 1093-1119.

[11] Meyers, M.A.; Chen, P.Y.; Lopez, M.I.; Seki, Y.; Lin, A.Y.M. Biological materials: A materials science approach. *J. Mech. Behav. Biomed. Mater.,* **2011**, *4*(5), 626-657.

[12] Currey, J.D. Hierarchies in Biomineral Structures. *Science (80-).* **2005**, *309*(5732), 253-254.

[13] Bose, S.; Vahabzadeh, S.; Bandyopadhyay, A. Bone tissue engineering using 3D printing. *Mater. Today,* **2013**, *16*(12), 496-504.

[14] Minas, C.; Carnelli, D.; Tervoort, E.; Studart, A.R. 3D printing of emulsions and foams into hierarchical porous ceramics. *Adv. Mater.,* **2016**, *28*(45), 9993-9999.

[15] Wegst, U.G.K.; Ashby, M.F. The mechanical efficiency of natural materials. *Philos. Mag.,* **2004**, *84*(21), 2167-2181.

[16] D'Alessandro, D.; Perale, G.; Milazzo, M.; Moscato, S.; Stefanini, C.; Pertici, G.; Danti, S. Bovine bone matrix/poly(l-lactic-co-ε-caprolactone)/gelatin hybrid scaffold (SmartBone®) for maxillary sinus augmentation: A histologic study on bone regeneration. *Int. J. Pharm.,* **2017**, *523*(2), 534-544.

[17] Pertici, G.; Rossi, F.; Casalini, T.; Perale, G. Composite polymer-coated mineral grafts for bone regeneration: Material characterisation and model study. *Ann. oral Maxilofac. Surg.,* **2014**, *2*(1), 1-7.

[18] Campana, V.; Milano, G.; Pagano, E.; Barba, M.; Cicione, C.; Salonna, G.; Lattanzi, W.; Logroscino, G. Bone substitutes in orthopaedic surgery: From basic science to clinical practice. *J. Mater. Sci. Mater. Med.,* **2014**, *25*(10), 2445-2461.

[19] Knöfler, W.; Barth, T.; Graul, R.; Krampe, D. Retrospective analysis of 10,000 implants from insertion up to 20 years-analysis of implantations using augmentative procedures. *Int. J. Implant Dent.,* **2016**, *2*(1), 25.

[20] Sarkar, S.K.; Lee, B.T. Hard tissue regeneration using bone substitutes: An update on innovations in materials. *Kor. J. Intern. Med.,* **2015**, *30*, 279-293.

[21] Athanasiou, V.T.; Papachristou, D.J.; Panagopoulos, A.; Saridis, A.; Scopa, C.D.; Megas, P. Histological comparison of autograft, allograft-dbm, xenograft, and synthetic grafts in a trabecular bone defect: An experimental study in rabbits. *Med. Sci. Monit.,* **2010**, *16*(1), BR24-R31.

[22] Datta, A.; Gheduzzi, S.; Miles, A.W. A comparison of the viscoelastic properties of bone grafts. *Clin. Biomech.,* **2006**, *21*(7), 761-766.

[23] Planell, J.A. *Bone Repair Biomaterials*; Woodhead Publishing Limited, 2009.

[24] Roato, I.; Belisario, D.C.; Compagno, M.; Verderio, L.; Sighinolfi, A.; Mussano, F.; Genova, T.; Veneziano, F.; Pertici, G.; Perale, G.; Ferracini, R. Adipose-derived stromal vascular fraction/xenohybrid bone scaffold: An alternative source for bone regeneration. *Stem Cells Int.,* **2018**, *2018*.

[25] Langton, C.M.; Njeh, C.F. *The Physical Measurement of Bone*; Institute of Physics Publishing Bristol and Philadelphia, 2003.

[26] Skedros, J.G.; Baucom, S.L. Mathematical analysis of trabecular "trajectories" in apparent trajectorial structures: The unfortunate historical emphasis on the human proximal femur. *J. Theor. Biol.,* **2007**, *244*(1), 15-45.

[27] Zioupos, P.; Cook, R.B.; Hutchinson, J.R. Some basic relationships between density values in cancellous and cortical bone. *J. Biomech.,* **2008**, *41*(9), 1961-1968.

[28] Ceccarelli, G.; Presta, R.; Benedetti, L.; Cusella De Angelis, M.G.; Lupi, S.M.; Rodriguez, Y.; Baena, R. Emerging perspectives in scaffold for tissue engineering in oral surgery. *Stem Cells Int.,* **2017**, *2017*.

[29] Colaço, H.B.; Shah, Z.; Back, D.; Davies, A.; Ajuied, A. Xenograft in orthopaedics. *Orthop. Trauma,* **2015**, *29*(4), 253-260.

[30] Stacchi, C.; Lombardi, T.; Ottonelli, R.; Berton, F.; Perinetti, G.; Traini, T. New bone formation after transcrestal sinus floor elevation was influenced by sinus cavity dimensions: A prospective histologic and histomorphometric study. *Clin. Oral Implants Res.,* **2018**, 465-479.

[31] Cingolani, A.; Casalini, T.; Caimi, S.; Klaue, A.; Sponchioni, M.; Rossi, F.; Perale, G. A methodologic approach for the selection of bio-resorbable polymers in the development of medical devices: The case of poly(l-lactide-co-ε-caprolactone). *Polymers (Basel).* **2018**, *10*(8), 851.

[32] Schrieber, R.; Herbert, G. *Gelatine Handbook: Theory and Industrial Practice*; Wiley, Ed.; UK, 2007.

[33] Pertici, G. Bone implant matrix and method of preparing the same. WO2010070416A1, 2010.

[34] Pertici, G.; Carinci, F.; Carusi, G.; Epistatus, D.; Villa, T.; Crivelli, F.; Rossi, F.; Perale, G. Composite polymer-coated mineral scaffolds for bone regeneration: From material characterization To

Human Studies. *J. Biol. Regul. Homeost. Agents,* **2015**, *29*(3 Suppl 1), 136-148.

[35] Eliceiri, K.; Schneider, C.A.; Rasband, W.S.; Eliceiri, K.W. NIH image to image J: 25 years of image analysis historical commentary nih image to imageJ: 25 Years of image analysis. *Nat. Methods,* **2012**, *9*(7), 671-675.

[36] Schindelin, J.; Rueden, C.T.; Hiner, M.C.; Eliceiri, K.W. The imageJ ecosystem: An open platform for biomedical image analysis. *Mol. Reprod. Dev.,* **2015**, *82*, 518-529.

[37] Reznikov, N.; Chase, H.; Brumfeld, V.; Shahar, R.; Weiner, S. The 3D structure of the collagen fibril network in human trabecular bone: Relation to trabecular organization. *Bone,* **2015**, *71*, 189-195.

[38] Florencio-Silva, R.; Sasso, G.R.D.S.; Sasso-Cerri, E.; Simões, M.J.; Cerri, P.S. Biology of bone tissue: structure, function, and factors that influence bone cells. *Biomed. Res. Int.,* **2015**, *2015*.

[39] Alghadir, A.H.; Gabr, S.A.; Al-Eisa, E. Physical activity and lifestyle effects on bone mineral density among young adults: Sociodemographic and biochemical analysis. *J. Phys. Ther. Sci.,* **2015**, *27*(7), 2261-2270.

[40] Chen, P.Y.; McKittrick, J. Compressive mechanical properties of demineralized and deproteinized cancellous bone. *J. Mech. Behav. Biomed. Mater.* **2011**, *4*(7), 961-973.

[41] Wolff, J. *Uber Die Innere Architektur Der Knochen Und Ihre Bedeutung Fuer Die Frage Vom Knochenwachstum*; Berlin□: Druck und Verlag von Georg Reimer, 1870.

[42] Bonfield, W.; Grynpas, M.D. Anisotropy of the Yound's Modulus of Bone. *Nature,* **1977**, *270*, 453-454.

[43] Töyräs, J.; Kröger, H.; Jurvelin, J.S. Bone properties as estimated by mineral density, ultrasound attenuation, and velocity. *Bone,* **1999**, *25*(6), 725-731.

[44] Joschek, S.; Nies, B.; Krotz, R.; Göpferich, A. Chemical and physicochemical characterization of porous hydroxyapatite ceramics made of natural bone. *Biomaterials,* **2000**, *21*(16), 1645-1658.

[45] Milne, A. J. B.; Amirfazli, A. The cassie equation: How it is meant to be used. *Adv. Colloid Interface Sci.,* **2012**, *170*(1-2), 48-55.

[46] Cassie, B.D.; Baxter, S. Wettability of porous surfaces. *Trans. Faraday Soc.,* **1944**, *40*(5), 546-551.

[47] Bormashenko, E. Progress in understanding wetting transitions on rough surfaces. *Adv. Colloid Interface Sci.,* **2015**, *222*, 92-103.

[48] Laguta, I.V; Stavinskaya, O.N.; Kuzema, P.A.; Kazakova, O.A.; Nasedkin, D.B. Hybrid materials on the basis of gelatin and hydrophilic-hydrophobic silica. *Prot. Met. Phys. Chem. Surfaces,* **2017**, *53*(5), 807-811.

[49] Launey, M.E.; Buehler, M.J.; Ritchie, R.O. On the mechanistic origins of toughness in bone. *Annu. Rev. Mater. Res.,* **2010**, *40*(1), 25-53.

[50] Mirkhalaf, M.; Khayer Dastjerdi, A.; Barthelat, F. Overcoming the brittleness of glass though bioinspiration and micro-architecture. *Nat. Commun.,* **2014**, *5*, 3166.

[51] Hannink, G.; Arts, J.J.C. Bioresorbability, porosity and mechanical strength of bone substitutes: What is optimal for bone regeneration? *Injury,* **2011**, *42*(Suppl. 2), S22-S25.